Results in Physics 10 (2018) 772–776

Contents lists available at ScienceDirect

Results in Physics

journal homepage: www.elsevier.com/locate/rinp

# Glow curve analysis of glassy system dosimeter subjected to photon and electron irradiations

M.H.A. Mhareb[a], M. Maghrabi[b], Y.S.M. Alajerami[c,*], S. Hashim[d], S.K. Ghoshal[d], M.A. Saleh[e], K.M. Abushab[c]

[a] Department of Physics, College of Science, Imam Abdulrahman Bin Faisal University, P.O. Box 1982, 31441 Dammam, Saudi Arabia
[b] Physics Department, Hashemite University, P.O. Box 150459, Zarqa 13115, Jordan
[c] Department of Medical Radiography, Al-Azhar University, Gaza Strip, Palestine
[d] Department of Physics, Faculty of Science, Universiti Teknologi Malaysia, 81310 UTM Skudai, Johor, Malaysia
[e] Nuclear Engineering Programme, Faculty of Petroleum and Renewable Energy Engineering, Universiti Teknologi Malaysia, 81310 Skudai, Johor, Malaysia

ARTICLE INFO

*Keywords:*
Dosimeter
Analysis
Boron

ABSTRACT

The current paper illustrates glow curve analysis of newly developed Borate glass dosimeters. A series of dosimetric properties including dose response for photons and electrons, energy response, optical fading, and precision were determined. Glow curve deconvolution based on the general order kinetics equation was applied to extract the trapping parameters. Excellent fitting was obtained with the superposition of three-second order glow peaks. The quality of fitting was monitored through the $r^2$ value which is always in excess of 0.9998. Thermoluminescence (TL) measurements showed that the material exhibits good linear dose–response over the delivered range of absorbed dose from 0.5 to 4 Gy for photons and electrons irradiation with low energy dependence. The material exhibits large signal loss when exposed to direct sunlight and moderate signal loss when exposed to fluorescent light. Therefore, it is recommended to use the current dosimeters indoor and to avoid prolonged direct exposure to fluorescent light. This combination of properties makes the material suitable for radiation dosimetry.

## Introduction

Thermoluminescence (TL) is the phenomenon of light emission from dielectric or semiconducting materials that are formerly subjected to ionizing radiation under circumstances of increased temperature. Thermoluminescent materials or phosphors have the feature of taking up and storing energy in traps when it is subjected to ionizing radiation. Afterward, this energy is liberated from these traps by heating the material with the production of light. The intensity of the emitted light depends on the nature and the quantity of impurities (dopants); the size of component particles of material, the network of defects present in the material, and the effect of radiation interaction [1–4].

Glow Curve is a spectrum produced to clarify the relation between the temperature used for releasing the trapped electrons and the intensity of the emitted light after the recombination of the released electrons [5,6]. Several studies have been conducted on borate glass to interpret its glow curve by using different compositions (dopants) [7,8]. The three parameter model is one of the most convenient models (Peak shape methods) that extensively developed by Chen 1969 [9,10]. According to Peak Shape Method, TL is described by three parameters namely activation energy ($E$), the order of kinetics ($b$) and frequency factor ($s$). Several methods have been developed to extract the trap parameters from the TL glow curve. Methods that are frequently used in the analysis include: peak shape methods, initial rise method, various heating rates method and curve-fitting [11].

Borates dosimeters showed attractive properties due to their tissue equivalent, good linearity, high sensitivity to external dose, low cost, and the ease with which they can be prepared [12,13]. Conversely, the hygroscopic nature of borate glass negatively affects its performance. Intensive research has been dedicated to improve the stability and to enhance the sensitivity by using different types of metals (alkali/alkaline earth) as a modifier, transition metals, and rare earth(s) as dopants (co-dopants) [7,14,15]. We used lithium as a modifier to act on a vacancy creator by increasing dislocation and improving the strength of the host. In contrast, lithium ions have a closed structure with no energy levels within 10 eV, and are expected to provide luminescence activation especially at high doses [16]. We add magnesium oxide to the lattice not only to enhance the strength of the glass network but also

* Corresponding author.
*E-mail address:* yasser_ajr@hotmail.com (Y.S.M. Alajerami).

https://doi.org/10.1016/j.rinp.2018.07.033
Received 16 June 2018; Received in revised form 24 July 2018; Accepted 25 July 2018
Available online 30 July 2018

to increase the sensitivity of the material [17]. In this study, we are trying to illustrate the dosimetric properties of a newly proposed borate composition. This paper is a continuation of our previous studies that showed optimistic TL properties of the proposed dosimeters [8,18–20].

## Experiments

### *Sample preparation*

Samples were prepared by the conventional melt-quench method. High purity raw materials (purchased from Sigma-Aldrish) of boron oxide (glass former), lithium and magnesium oxides (modifier), dysprosium and phosphors oxides as co-dopants where mechanically mixed for 24 h. The mixture was melted in an alumina crucible at 1200 °C for 45 min using the electrical furnace. To avoid bubbles formation, frequent stirring for crucibles during the fusion process. The molten was then poured into steel in another furnace at a temperature of 350 °C for 3 h. Finally, the temperature was gradually reduced to room temperature with a cooling rate of 10 °C $min^{-1}$. Table 1 lists the chemical data composition of the prepared glasses.

In the current study, two series of glass with stoichiometric compositions were synthesized to study the effect of the co-dopant on the TL response as follows:

Series 1: 20 $Li_2O$: $(70-x)$ $B_2O_3$: 10 MgO: $x-Dy_2O_3$, $0.3 \le x \le 1$ and
Series 2: 20 $Li_2O$: $(69.5-y)$ $B_2O_3$: 10 MgO: $0.5-Dy_2O_3$: $y-P_2O_5$, $0.5 \le y \le 2$,

Previous studies on this composition was conducted by our group showed that the highest TL output is for G2 and G6 (optimum concentration) [8,18–20].

### *Samples irradiation*

The irradiation process was performed by various radiation sources such as x-rays, gamma rays, photons of LINAC, and electrons with different energies and doses. TL measurements were conducted in the Secondary Standard Dosimetry Lab (SSDL) at the Malaysian Nuclear Agency using Harshow TLD reader (4500). Full details about the reading process were mentioned in previous study [20]. Glow curves were collected after 24 h of irradiation to reduce/eliminate the spurious thermoluminescence signals. Samples were stored in a dark place at ambient temperature to avoid any influence of background light. The average of three to five samples was calculated for each irradiation and readout process.

## Results and discussion

### *Glow curve analysis*

The glow curves of LMB:Dy (G2) and LMB:Dy,P (G6) were deconvoluted using the general order kinetics expression, namely

$$I = s\, n_o \exp(-E/kT)\left[1 + \left(\frac{s\,(b-1)}{\beta}\right)\int_{T_o}^{T} \exp(-E/kT')\,dT'\right]^{\frac{-b}{b-1}} \quad (1)$$

where $\beta$ is the constant heating rate, $b$ is the order of kinetics and $s = s'' n_0^{(b-1)}$. With this definition, $s$ has the units of frequency ($s^{-1}$) similar to that in the first order kinetics, but it depends on the applied dose rather than being a constant. Eq. (1) includes the second order kinetics ($b = 2$) and reduces to the first order kinetics ($b = 1$) when $b \to 1$. Since $b$ is one of the unknown parameters we decided to use the general order kinetics with $b$ may take any value between 1 and 2.

Glow curve fitting was conducted using the commercial PeakFit program. The program has the ability to deconvolute composite peak into its individual components using the predefined functions (say Gaussian). In addition, the user has the facility to define and install his/her function using the User-Defined Functions (UDF) option. Eq. (1) was installed into PeakFit's equation set using the User-Defined Functions (UDF) option [21]. The fitting process started with one peak only with $E$, $b$ $s$ and $n_o$ as free parameters. The program starts to vary these parameters within the predefined range of each parameter in an iterative manner to minimize the error between the experimental curve and the calculated one. The fitting process stops when self-constancy is reached or when the fitting is failed. It should be mentioned here that it was not possible to fit the experimental curve with a single peak of any order which indicates that the apparently "single peak" is, in fact, a complex of strongly overlapping peaks. The fitting was first tried using a superposition of first-order glow peaks. We started with two peaks and depending on the quality of fit another peak is added each time. No satisfactory fitting was obtained in this case. The data were then fitted to the general order kinetics expression. Following the same procedure as already mentioned excellent fitting was obtained with the superposition of three second-order glow peaks. The fitting process was repeated three times by varying the input parameters to check the constancy of the obtained parameters. In each trial, the program was able to produce the same values of the trapping parameters within ± 2%. Increasing the number of peaks did not enhance the quality of fitting. The quality of fitting was monitored through the $r^2$ value, which is always in excess of 0.9998.

Figs. 1 and 2 show the TL yields of G2 and G6 together with their deconvoluted peaks and the sum of the individual components. Obviously, the addition of phosphorus makes the glow curve broader and shifts the whole TL complex to higher temperatures. The presence of phosphorus did not introduce new traps as the two materials were fitted by the same number of peaks. Its presence is mainly sensed by the frequency factor values where an increase of one order of magnitude was observed. The effect of adding phosphorus as a co-dopant on the trap depth is rather minimal with no change in the order of kinetics. Table 2 illustrates the trapping parameters of the individual peaks for one sample of each type. It is interesting to note that all the individual peaks were fitted with second order kinetics and minimal change in the activation energy. The variation occurs solely in the frequency factor. This indicates that (1) the retrapping process dominates the recombination process in this material. (2) the material may have very closely overlapping trapping levels with a distribution of frequency factors.

**Table 1**
The detailed compositions of the studied glass samples.

| Glass Code | Composition (mol%) | | | | |
|---|---|---|---|---|---|
| | $Li_2O$ | $B_2O_3$ | MgO | $Dy_2O_3$ | $P_2O_5$ |
| G1 | 20% | 69.7% | 10% | 0.3% | – |
| *G2* | *20%* | *69.5%* | *10%* | *0.5%* | – |
| G3 | 20% | 69.3% | 10% | 0.7% | – |
| G4 | 20% | 69.0% | 10% | 1.0% | – |
| G5 | 20% | 69.0% | 10% | 0.5% | 0.5% |
| *G6* | *20%* | *68.5%* | *10%* | *0.5%* | *1.0%* |
| G7 | 20% | 68.0% | 10% | 0.5% | 1.5% |
| G8 | 20% | 67.5% | 10% | 0.5% | 2.0% |

### *Photon dose response*

The linearity of the proposed dosimeters was checked at two energies (6 and 10 MV) obtained from a linear accelerator machine. Fig. 3 shows the photon dose response of G2 and G6 within the dose range of 0.5 to 4 Gy. Promising dose linearity with good linear correlation coefficient is achieved. The gradient linear fit at 6 MV is $2.7303 \times 10^4$ nC.$Gy^{-1}$ for G2 and $5.0176 \times 10^4$ nC.$Gy^{-1}$ for G6.

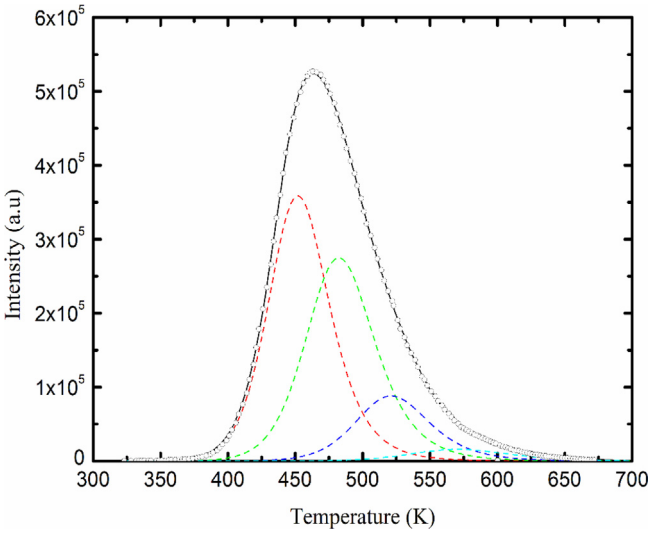


**Fig. 1.** Glow curve deconvolution of G2.

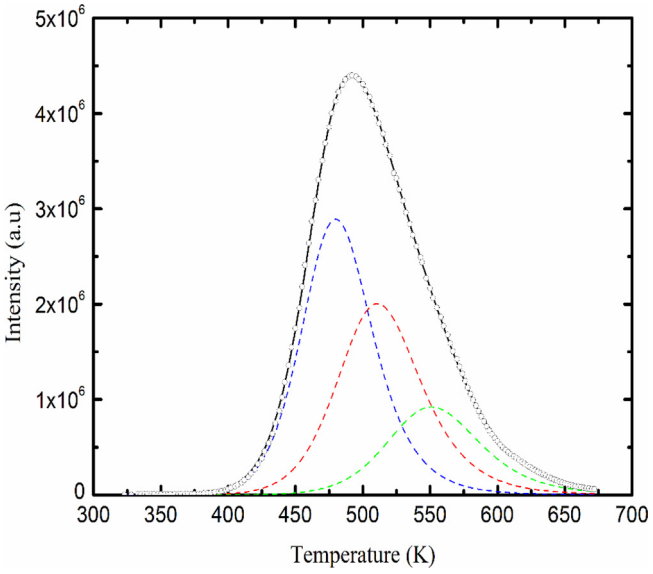


**Fig. 2.** Glow curve deconvolution of G6.

**Table 2**
TL trapping parameters for G2 and G6 samples obtained by curve fitting.

| Samples | Peak No. | $T_m$ (K) | Activation energy (eV) | Frequency factor ($s^{-1}$) | Kinetic order (b) |
|---|---|---|---|---|---|
| G2 | 1 | 435 | 1.06 | $3.0 \times 10^{10}$ | 2 |
| | 2 | 470 | 1.01 | $1.9 \times 10^{9}$ | 2 |
| | 3 | 525 | 1.06 | $8.8 \times 10^{8}$ | 2 |
| G6 | 1 | 460 | 1.10 | $5.2 \times 10^{11}$ | 2 |
| | 2 | 515 | 1.10 | $8.0 \times 10^{10}$ | 2 |
| | 3 | 550 | 1.20 | $9.4 \times 10^{10}$ | 2 |

*Electron dose response*

The electron response of the proposed dosimeters was checked by performing measurements at energy 6 MeV. Fig. 3 exhibits good linearity with good correlation coefficient. The gradient of the linear fit at 6 MeV is $3.1734 \times 10^4$ nC.Gy$^{-1}$ for G2 and $5.6662 \times 10^4$ nC.Gy$^{-1}$ for G6. It is clear that the photon and electron dose response of G6 is ~2 times higher than that of G2.

The difference in the TL yield for photons or electrons irradiation

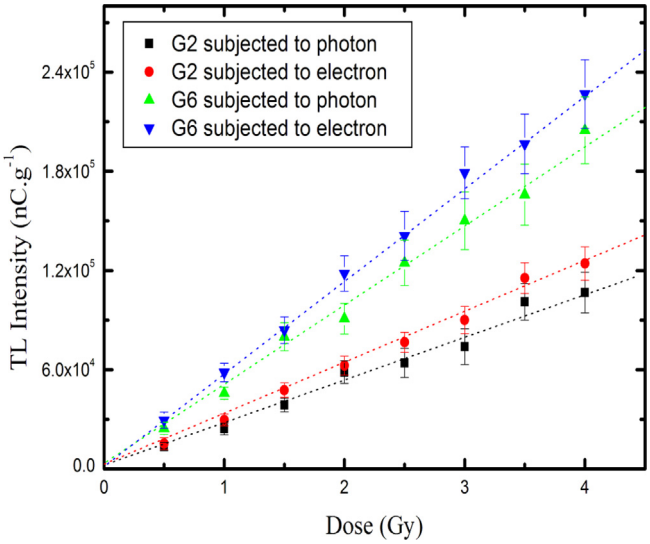


**Fig. 3.** Dose response of G2 and G6 subjected to photon and electron from LINAC irradiation at 6 MV and 6 MeV.

shows that the electron response is higher than the photon response by a factor of 1.16 and 1.21 for G6 and G2, respectively. This can be attributed to the greater linear energy transfer (LET) for electrons [22,23].

*Energy response*

The photon energy response *S(E)* was determined theoretically and experimentally. *S(E)* can simply be calculated as the ratio between the mass energy absorption coefficients of the TL material and air respectively, within the energy range up to 3 MeV. *S(E)* is defined as:

$$S(E) = \frac{\left(\frac{\mu_{en}}{\rho}\right)_m}{\left(\frac{\mu_{en}}{\rho}\right)_{ref}} \quad (2)$$

In the current calculation, air is used as a reference medium for different reasons: (1) a well-defined quantity; (2) the exposure can simply and precisely be measured for it and (3) the ratio between the absorbed dose and exposure is constant.

The relative energy response (*RER*) is defined as the photon energy response at energy *E* over the energy response of photons from a $^{60}$Co source (Eq. (3)):

$$RER = \frac{S(E)}{S(E)_{60_{Co}}} \quad (3)$$

The prepared dosimeters are compound; hence the following rule of mixtures applies, namely:

$$\left(\frac{\mu_{en}}{\rho}\right)_m = \sum_i \left(\frac{\mu_{en}}{\rho}\right)_i \cdot W_i \quad (4)$$

where $\left(\frac{\mu_{en}}{\rho}\right)_i$ represents the mass energy absorption coefficient of element *i* and $W_i$ is the fraction by weight of the *i*th element.

Table 3 shows the *S(E)* and *RER* values determined experimentally and theoretically for G2 and G6. The plots of *S(E)* and *RER* for G2 and G6 are shown in Figs. 4 and 5, respectively.

The prepared dosimeters show a small hump at 40 keV. These results confirm that the dominant process in this range is the photoelectric effect. The *RER* at 40 keV for G2 and G6 are 1.16 and 1.20, respectively.

**Table 3**
Photon energy response and relative energy response for the proposed dosimeters.

| Energy (MeV) | Energy response *S(E)* | | Relative Energy Response (RER) | | | |
|---|---|---|---|---|---|---|
| | | | Theoretical | | Experimental | |
| | G2 | G6 | G2 | G6 | G2 | G6 |
| 0.04 | 1.14 | 1.31 | 1.19 | 1.36 | 1.16 | 1.20 |
| 0.06 | 1.14 | 1.26 | 1.20 | 1.31 | 1.15 | 1.17 |
| 0.08 | 1.09 | 1.15 | 1.14 | 1.20 | 1.05 | 1.08 |
| 0.10 | 1.04 | 1.07 | 1.09 | 1.12 | 1.03 | 1.05 |
| 0.15 | 9.86 | 9.97 | 1.03 | 1.04 | 1.01 | 1.01 |
| 1.25 | 9.56 | 9.58 | 1.00 | 1.00 | 1.00 | 1.00 |

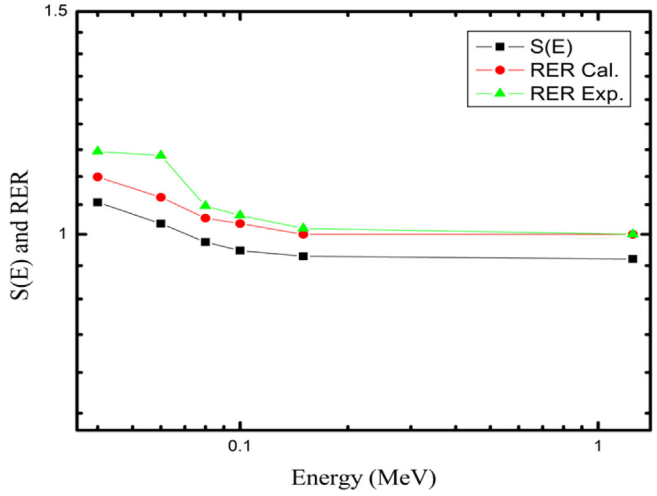


**Fig. 4.** Energy response and Relative energy response for G2.

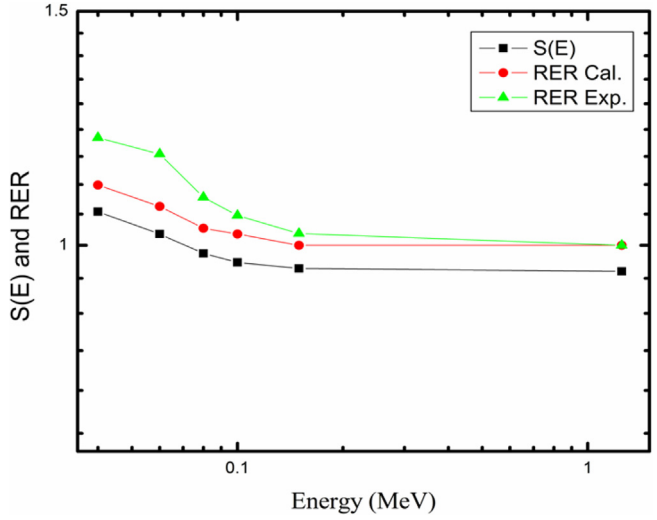


**Fig. 5.** Energy response and Relative energy response for G6.

*Optical fading and signal stability*

The stability of signal (trapped electrons) is essential to estimate the dosimeter performance. According to McKeever et al. [24], hygroscopic dosimeter, traps depth, storage temperature and heat treatment used for reading and pre-annealing have a direct effect on signal stability.

Thermal fading measurements of the current dosimeters were studied by our group in previous publications [8,20]. In the current work, optical fading (effect of sunlight and some specific light on the irradiated dosimeters) was examined. The proposed dosimeters exhibited high sensitivity to light. The large loss in the stored signal was observed as a result of exposing the samples to direct sunlight. A reduction of about 71% in the TL intensity of G2 was observed after 1 h and about 90% after 6 h as illustrated in Fig. 6. Regarding G6, the signal loss was about 73% after 1 h and about 93% after 6 h (Fig. 6).

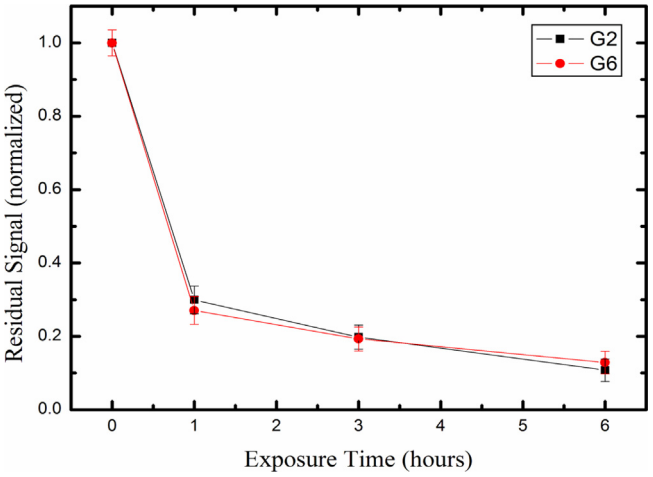


**Fig. 6.** Fading characteristics for G2 and G6 exposed to direct sunlight (3 Gy).

Furthermore, the current dosimeters were exposed to direct fluorescent light at 1 m for a period of one week. Fig. 7 displays the stability of the signal for G2 and G6 with the elapsed time. Both dosimeters exhibited a reduction in the stored signal of about 70% after 1 week.

It can be inferred here that exposing the current dosimeters for direct sunlight or fluorescent light is responsible for the loss of a large amount of the stored signal in these materials. Thus, it is recommended to cover both dosimeters with the radio-opaque material when utilized in dosimetric practice.

## Conclusion

The proposed dosimeters exhibited good dosimetric properties. The electrons response of the proposed dosimeters is higher than the photons response at different energies. This behavior is attributed to the different effect of LETs in electrons and photons interactions. It is recommended to use the new dosimeters indoor and to avoid prolonged direct exposure to fluorescent light. These promising dosimetric features suggest that the present TL dosimeters are potential for individual

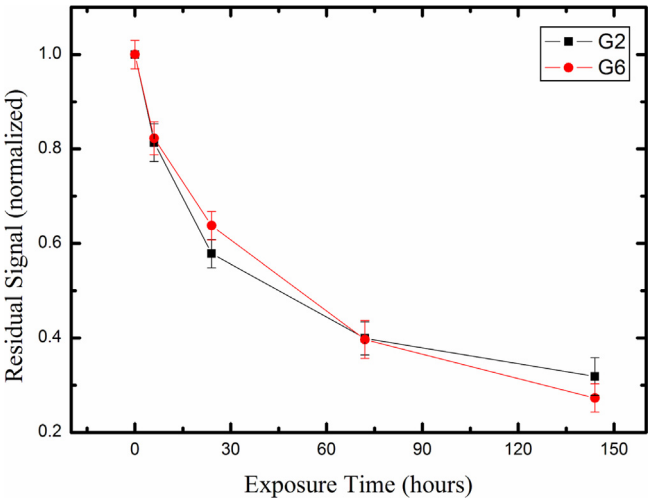


**Fig. 7.** Fading characteristics for G2 and G6 exposed to direct fluorescent light (3 Gy).

dose monitoring and medical applications.

## Acknowledgments

The authors are grateful to the Ministry of Education, Malaysia and Universiti Teknologi Malaysia (UTM) for providing a financial assistance through the Research University/Flagship Grant Scheme (vote number 17H79 and 03G72).

## References

[1] Kitis G, Gomez-Ros JM. Thermoluminescence glow-curve deconvolution functions for mixed order of kinetics and continuous trap distribution by Nuclear Instruments and Methods. Nucl Instr Meth Phys Res B 2000;440:224–31.
[2] Boronat C, Rivera T, García-Guinea J, Correcher V. Cathodoluminescence emission of REE (Dy, Pr and Eu) doped $LaAlO_3$ phosphors. Radiat Phys Chem 2017;130:236–42.
[3] Roman-Lopez J, Correcher V, Garcia-Guinea J, Rivera T, Lozano IB. Cathodoluminescence and green-thermoluminescence response of $CaSO_4$: Dy, P films. J Lumin 2013;135:89–92.
[4] Barrera-Villatoro A, Boronat C, Rivera-Montalvo T, Correcher V, García-Guinea J, Zarate-Medina J. Cathodoluminescence response of natural and synthetic lanthanide-rich phosphates ($Ln^{3+}$: Ce, Nd). Radiat Phys Chem 2017;141:271–5.
[5] Furetta C. Handbook of thermoluminescence. Singapore: World Scientific Pub; 2003.
[6] Pekpak E, Yilmaz A, Ozbayoglu G. An overview on preparation and TL characterization of lithium borates for dosimetric use. Open Min Proc J 2010;3(1):14–24.
[7] Alajerami YSM, Hashim S, Ramli AT, Saleh MA, Kadni T. Thermoluminescence properties of $Li_2CO_3$–$K_2CO_3$–$H_3BO_3$ glass system co-doped with CuO and MgO. Radiat Protect Dosim 2012;155(1):1–10.
[8] Mhareb MHA, Hashim S, Ghoshal SK, Alajerami YSM, Saleh MA, Azizan SAB, et al. Influences of dysprosium and phosphorous oxides co-doping on thermoluminescence features and kinetic parameters of lithium magnesium borate glass. J Radiol Nucl Chem 2015;305(2):469–77.
[9] Chen R. On the calculation of activation energies and frequency factors from glow curves. J Appl Phys 1969;40:570–85.
[10] Chen R. Glow curves with general order kinetics. J Electrochem Soc 1969;116:1254–7.
[11] Chen R, Mckeever SWS. Theory of Thermoluminescence and related phenomena. Singapore: World Scientific; 1997.
[12] Hashim S, Alajerami YSM, Ramli AT, Ghoshal SK, Saleh MA, Kadir AA, et al. Thermoluminescence dosimetry properties and kinetic parameters of lithium potassium borate glass co-doped with titanium and magnesium oxides. Appl Radiat Isot 2014;91:126–30.
[13] Mhareb MHA, Hashim S, Ghoshal SK, Alajerami YSM, Bqoor MJ, Hamdan AI, et al. Effect of $Dy_2O_3$ impurities on the physical, optical and thermoluminescence properties of lithium borate glass. J Lumin 2016;177:366–72.
[14] Liu L, Zhang Y, Hao J, Li C, Wang S, Su Q. Thermoluminescence studies of $LiBa_2B_5O_{10}$: $RE^{3+}$ (RE= Dy, Tb and Tm). J Phys Chem Solids 2007;68(9):1745–8.
[15] Jiang LH, Zhang YL, Li CY, Hao JQ, Su Q. Thermoluminescence studies of $LiSrBO_3$: $RE^{3+}$ (RE= Dy, Tb, Tm and Ce). Appl Radiat Isot 2010;68(1):196–200.
[16] Rao RB, Gerhardt RA, Veeraiah N. Spectroscopic characterization, conductivity and relaxation anomalies in the $Li_2O$–MgO–$B_2O_3$ glass system: effect of nickel ions. J Phys Chem Solids 2008;69(11):2813–26.
[17] Kenneth WW, Kenneth GD, Raymond DE. General Chemistry. third ed. Philadelphia, PA: Saunders College Publishing; 1988.
[18] Hashim S, Mhareb MHA, Ghoshal SK, Alajerami YSM, Bradley DA, Saripan MI, Tamchek N, Alzimami K. Luminescence characteristics of $Li_2O$–MgO–$B_2O_3$ doped with $Dy^{3+}$ as a solid TL detector. Radiat Phys Chem 2015;116:138–41.
[19] Mhareb MHA, Hashim S, Ghoshal SK, Alajerami YSM, Saleh MA, Razak NAB, et al. Thermoluminescence properties of lithium magnesium borate glasses system doped with dysprosium oxide. Lumin 2015;30(8):1330–5.
[20] Hashim S, Mhareb MHA, Ghoshal SK, Alajerami YSM, Saripan MI, Bradley DA. Luminescence features of dysprosium and phosphorus oxide co-doped lithium magnesium borate glass. Radiat Phys Chem 2017;137:45–8.
[21] Maghrabi M, Arafah DE. Sensitization of the thermoluminescence response of CaF2 phosphors. Phys Status Solidi (a) 2003;195(2):459–67.
[22] Alajerami YSM, Hashim S, Ramli AT, Saleh MA, Saripan MI, Alzimami K, Ung NM. Thermoluminescence responses of photon-and electron-irradiated lithium potassium borate co-doped with Cu + Mg or Ti + Mg. Appl Radiat Isot 2013;78:21–5.
[23] Hashim S, Al-Ahbabi S, Bradley DA, Webb M, Jeynes C, Ramli AT, Wagiran H. The thermoluminescence response of doped $SiO_2$ optical fibres subjected to photon and electron irradiations. Appl Radiat Isot 2009;67(3):423–7.
[24] McKeever SWS, Moscovitch M, Townsend PD. thermoluminescence dosimetry materials: properties and uses, nuclear. Kent: Technology Publishing; 1995.